JOURNAL OF Materials CHEMISTRY

Structure and properties of novel $M(dmit)_2$ salts with the Me_3N^+-TEMPO cation radical (Me_3N^+-TEMPO = *N*,*N*,*N*-trimethyl(1-oxyl-2,2,6,6-tetramethylpiperidin-4-yl)ammonium)†

Shuji Aonuma,*[a]‡ Hélène Casellas,[a] Christophe Faulmann,[a] Bénédicte Garreau de Bonneval,[a] Isabelle Malfant,*[a] Patrick Cassoux,*[a] Pascal G. Lacroix,[b] Yuko Hosokoshi[c] and Katsuya Inoue[c]

[a]*Equipe Précurseurs Moléculaires et Matériaux, LCC-CNRS, 205, Route de Narbonne, 31077 Toulouse, Cedex 04, France. E-mail: aonuma@lcc-toulouse.fr, cassoux@lcc-toulouse.fr*
[b]*Equipe Matériaux Moléculaires et Biomimétiques, LCC-CNRS, 205, Route de Narbonne, 31077 Toulouse, Cedex 04, France*
[c]*Institute for Molecular Science, Myodaiji, Okazaki, 444–8585, Japan*

Received 9th August 2000, Accepted 24th October 2000
First published as an Advance Article on the web 12th December 2000

Salts of the Me_3N^+-TEMPO cation radical (Me_3N^+-TEMPO = *N*,*N*,*N*-trimethyl(1-oxyl-2,2,6,6-tetramethylpiperidin-4-yl)ammonium) with I^- and PF_6^- are prepared. Their crystal structure and magnetic properties are reported (antiferromagnetically coupled dimers for (Me_3N-TEMPO)I and antiferromagnetically coupled chains for (Me_3N-TEMPO)PF_6). The Me_3N^+-TEMPO magnetic cation radical is associated with $M(dmit)_2$ (M = Ni, Pd; $dmit^{2-}$ = 1,3-dithiole-2-thioxo-4,5-dithiolato) to afford the divalent (Me_3N-TEMPO)$_2$[$M(dmit)_2$] (M = Ni, Pd) salts and the monovalent (Me_3N-TEMPO)[$Ni(dmit)_2$] salt. The crystal structures of (Me_3N-TEMPO)$_2$[$M(dmit)_2$] (M = Ni, Pd) and (Me_3N-TEMPO)[$Ni(dmit)_2$] are determined. In the (Me_3N-TEMPO)$_2$[$M(dmit)_2$] salts, a unique, non planar, chair conformation of the $M(dmit)_2$ molecule is observed. These salts display conventional Curie behaviour. The (Me_3N-TEMPO)[$Ni(dmit)_2$] salt exhibits a single-crystal room-temperature conductivity of 4×10^{-3} S cm^{-1}, which is rather high for an integral oxidation state salt.

Introduction

Co-existence or interplay of conductivity and magnetism is of great current interest in molecule-based material science.[1] Two different types of mechanism for this interplay can be considered: (1) magnetic coupling *via* an indirect exchange interaction through the conduction electrons;[2,3] (2) interaction of conduction electrons through magnetically ordered spins.[4] The most interesting results recently obtained along this line concern the characterisation of a paramagnetic superconductor, β″-(BEDT-TTF)$_4$(H_3O)[$Fe(C_2O_4)_3$]·(C_6H_5CN) (BEDT-TTF = bis(ethylenedithio)tetrathiafulvalene),[5] the first observation of a magnetic field-induced restoration of a highly conducting state in the λ-$(BETS)_2FeCl_4$ phase (BETS = bis-(ethylenedithio)tetraselenafulvalene),[6] and the preparation of the first antiferromagnetic superconductor, κ-$(BETS)_2FeBr_4$.[7]

For such purposes, some of the advantages in using molecule-based materials may be recollected as follows: First, their crystal lattice is constructed with molecules that can be extensively and minutely modified by synthetic methods. Second, in most cases, molecules are connected by van der Waals interactions which are much weaker than ionic, covalent or metallic bonds. This means that a molecule-based crystal is *soft*, and that large effects can be expected by changing the temperature or applying pressure. Third, the molecular building blocks may have various degrees of freedom (*e.g.* conformational, rotational) which may result in a variety of structures, and hence, of physical properties. Fourth, and especially for planar systems, the frequently encountered low dimensionality of the structures often results in unusual physical properties such as spin density wave, charge density wave or spin–Peierls instabilities for the conducting properties, and spin ladder behaviour (quantum spin system) for the magnetic properties. Due to the rather weak intermolecular interactions, the tight-binding view of the electronic band structure is often well suited for understanding the mechanism of conducting properties. On the other hand, magnetism of *organic radicals* (in the narrow sense), where magnetic spins are isotropic because they originate from s and/or p electrons, can be rationalised in terms of the ideal Heisenberg spin system.

$M(dmit)_2$ ($dmit^{2-}$ = 1,3-dithiole-2-thioxo-4,5-dithiolato; Chart 1) is a planar acceptor molecule known as a precursor to charge-transfer salts exhibiting metal-like and even superconducting behaviour.[8,9] In other respects, after the discovery in 1985 of the first charge-transfer salt-based bulk ferromagnet, [$Fe(C_5Me_5)_2$](TCNE) (TCNE = tetracyanoethylene),[10] a great research effort has been devoted to the study of charge-transfer salts involving planar π acceptor anion radicals associated with paramagnetic cations,[9,11] including the first dmit-based bulk ferromagnet, [$Mn(C_5Me_5)_2$][$Ni(dmit)_2$].[12]

The first *purely organic* (*i.e.*, without magnetic d spins) bulk ferromagnet,[13] the nitronyl aminoxyl radical crystal phase, β-*p*-NPNN (*p*-NPNN = *p*-nitrophenyl nitronyl nitroxide[14]), was reported in 1991.[15] Other purely organic ferromagnets, such as diazaadamantanedioxyl[16] and several TEMPO derivatives

†The crystal structure of (Me_3N-TEMPO)$_2$[$M(dmit)_2$] (Fig. S1) and the molar magnetic susceptibility of (Me_3N-TEMPO)PF_6 (Fig. S2) are available as supplementary data. For direct electronic access see http://www.rsc.org/suppdata/jm/b0/b008424g/

‡Visiting research fellow from The Institute for Solid State Physics, The University of Tokyo, Kashiwa, Chiba 277-8581, Japan.

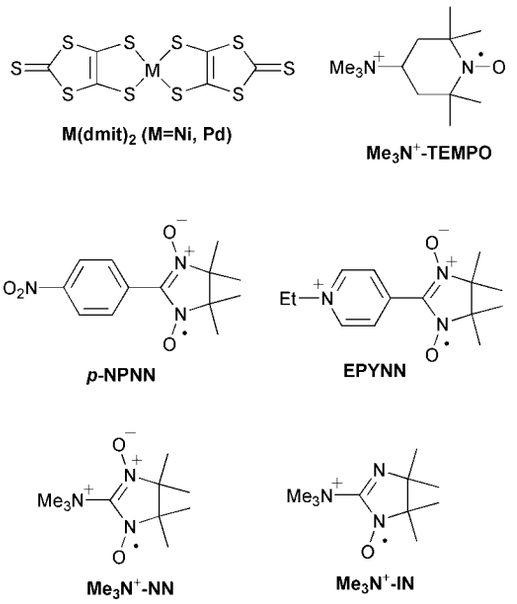

Chart 1

(TEMPO = 2,2,6,6-tetramethylpiperidin-1-oxyl),[17] have been reported. Charge-transfer salts based on organic radicals have also been extensively studied.[18] One of the most spectacular recent results obtained by using charge-transfer salts of organic radicals is the observation of a spin ladder behaviour in a nitronyl aminoxyl-pyridinium (EPYNN) salt of $Ni(dmit)_2$.[19] Charge-transfer salts of tetrathiafulvalene (TTF) donors bearing nitroxyl[20] radicals have been also reported.[21,22]

For promoting a possible interaction between conducting electrons and magnetic spins in a hybrid molecule-based system, the conducting and magnetic components should be geometrically located close to each other. Therefore, less sterically hindered and compact organic radicals should be more suitable for use as counter cations. For example, alkyl ammonium cations (*e.g.* Me_3N^+-TEMPO, *N*,*N*,*N*-trimethyl(1-oxyl-2,2,6,6-tetramethylpiperidin-4-yl)ammonium; see Chart 1) should be preferred to pyridinium cations such as EPYNN. Nitronyl or imino aminoxyl cations with small ammonio groups (*e.g.* Me_3N^+-NN, Me_3N^+-IN) may be even more attractive because of their small size and also because of the delocalisation of the radical spin in the nitronyl aminoxyl, which could possibly enhance intermolecular interaction.

In this paper, we report on the crystal structure and magnetic properties of (Me_3N-TEMPO)X salts (X = I, PF_6), which can be readily prepared, are very stable, and can be associated with $M(dmit)_2$ radical anions. We also describe the preparation, crystal structure, and magnetic properties of (Me_3N-TEMPO)$_x$[$M(dmit)_2$] (M = Ni, x = 2, 1; M = Pd, x = 2).

Results and discussions

Syntheses

(Me_3N-TEMPO)I was prepared by reductive amination of oxo-TEMPO to Me_2N-TEMPO, followed by methylation with MeI. (Me_3N-TEMPO)PF_6 was prepared from (Me_3N-TEMPO)I by anion exchange with KPF_6 (Scheme 1).

The (Me_3N-TEMPO)$_2$[$Ni(dmit)_2$] and (Me_3N-TEMPO)$_2$-[$Pd(dmit)_2$] divalent salts were obtained by a metathesis reaction of an excess of (Me_3N-TEMPO)I with the corresponding (n-Bu_4N)$_2$[$M(dmit)_2$] (M = Ni, Pd) (Method A in Scheme 2), which afforded single crystals suitable for X-ray structural analysis. A crystalline powder of (Me_3N-TEMPO)$_2$[$M(dmit)_2$] was also obtained by a similar metathesis

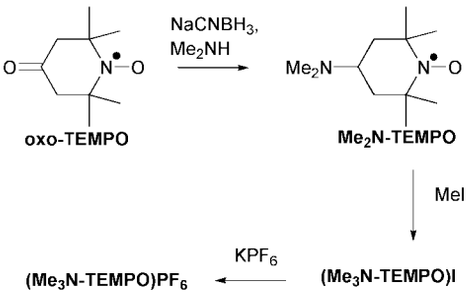

Scheme 1

reaction of equimolar (Me_3N-TEMPO)I with Na_2[$M(dmit)_2$] (M = Ni, Pd) (Method B).

Metathesis between Na[$Ni(dmit)_2$] and (Me_3N-TEMPO)I (Method C in Scheme 3) or iodine oxidation of the divalent (Me_3N-TEMPO)$_2$[$Ni(dmit)_2$] salt (Method D) afforded the monovalent (Me_3N-TEMPO)[$Ni(dmit)_2$], which is readily soluble in acetone or in acetonitrile.

In some cases, Method C simultaneously produced further oxidised species assumed to be (Me_3N-TEMPO)[$Ni(dmit)_2$]$_2$. This prompted us to study the redox behaviour of Me_3N^+-TEMPO to evaluate its potential oxidation ability. The cyclic voltammogram of (Me_3N-TEMPO)PF_6 measured in acetonitrile shows one pair of reversible waves. The half wave potential values at 0.92 V or 0.90 V *vs.* SCE were obtained by cyclic voltammetry (CV) or square wave voltammetry (SQW), respectively. With this last method, the half width of the peak corresponds to the transfer of one electron. In the case of (Me_3N-TEMPO)I, the redox potential was also *ca.* 0.9 V *vs.* SCE, with the corresponding wave overlapping with the $I^-/I^{\cdot}$ redox wave (0.86 V *vs.* SCE). Thus, given the oxidation potential observed for Me_3N^+-TEMPO, this radical cannot be considered as responsible for a possible further oxidation of (Me_3N-TEMPO)[$Ni(dmit)_2$].

Crystal structures

(Me_3N-TEMPO)I. Fig. 1 shows the molecular structure, together with the atomic labelling scheme, for the two independent Me_3N^+-TEMPO cations and the two I^- anions. The structure is formed by groups of four cations (A, B, A′, B′), in which the four oxygen atoms form a parallelogram (Fig. 2). The O···O distances are 4.578(6) between A and B′ and

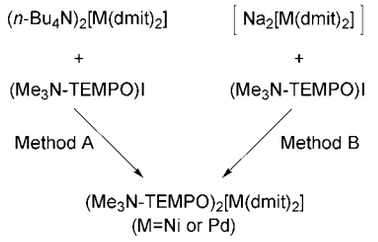

Scheme 2

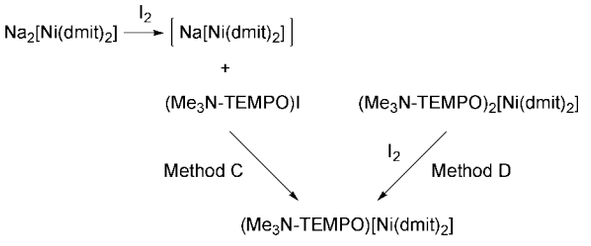

Scheme 3

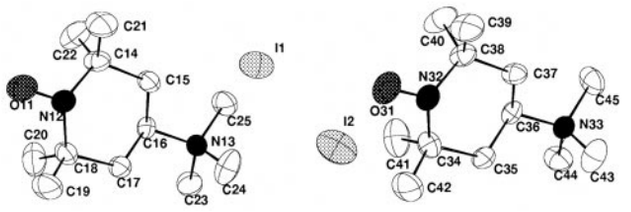

Fig. 1 Molecular structure and atom labelling scheme for (Me_3N-TEMPO)I.

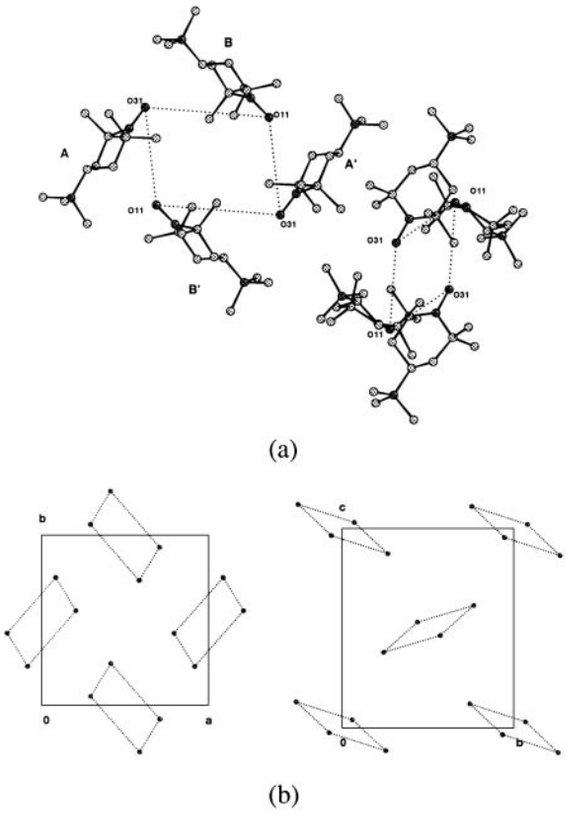

Fig. 2 (a) Projection of the structure of (Me_3N-TEMPO)I showing the parallelogram formed by the four cations. Dotted lines represent the O···O distances of 4.578(6) (AB′ and A′B) and 5.921(6) Å (AB and A′B′). (b) Projection of the structure of (Me_3N-TEMPO)I along the *a* and *c* axes showing the arrangement of the adjacent groups of oxygen atoms (only oxygen atoms are shown for clarity).

5.921(6) Å between A and B. The corresponding N···O distances are 3.789(6) Å and 5.024(6) Å, respectively (Fig. 2a). This may indicate that the interaction between A and B′ may be stronger than that between A and B, leading to a possible dimeric arrangement (see the section below on the magnetic properties of this compound). Within each group of four cations, the Me_3N^+-TEMPO cations (A and B, A′ and B, A and B′, A′ and B′; see Fig. 2)are perpendicular (angle

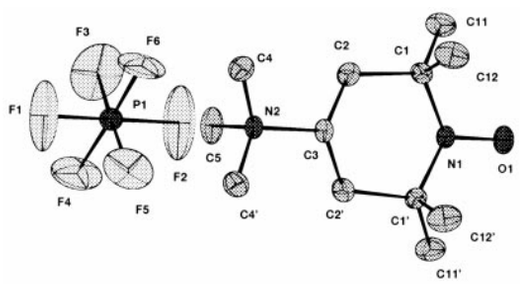

Fig. 3 Molecular structure and atom labelling scheme for (Me_3N-TEMPO)PF_6.

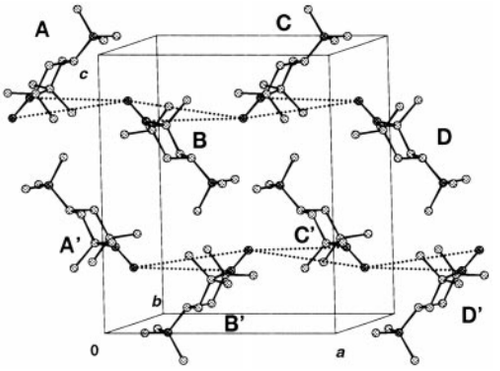

Fig. 4 Projection of the structure of (Me_3N-TEMPO)PF_6 showing two adjacent chains along the *a* axis (anions are omitted for clarity). Dotted lines represent the O···O distances of 5.7540(7) Å and the N···O distances of 4.827(3) Å.

between their mean planes (except H and Me) is 89.96(3)°) to each other. Six other groups of cations for which the oxygen planes form an angle of about 60° with the central plane (Fig. 2b) surround each A, B, A′, or B′ group along the [110] and [011] directions.

(Me_3N-TEMPO)PF_6. The molecular structure, together with the atom-labelling scheme, is shown in Fig. 3. The asymmetric unit contains one half Me_3N^+-TEMPO unit and one disordered PF_6^- unit, both lying on a mirror plane. Consequently, the unit cell contains four Me_3N^+-TEMPO cations and four PF_6^- anions. The structure consists of chains of cationic units, parallel to the *a* direction, with the anions lying in between (Fig. 4). Each chain (for example, …A–B–C–D… in Fig. 4) is built on Me_3N^+-TEMPO units perpendicular to each other (angle between their mean planes (except H and Me) is 90.41(4)°). Along the chains, the Me_3N^+-TEMPO units are connected through N···O and O···O interactions with interatomic distances of 4.827(3) and 5.7540(7) Å, respectively. The interatomic distances between atoms belonging to adjacent chains are much longer (>7.7 Å), indicating the absence of any interchain interactions.

(Me_3N-TEMPO)$_2$[M(dmit)$_2$] (M = Ni, Pd). The molecular structure of these two compounds, together with the atom-labelling scheme is shown in Fig. 5. These two compounds are isostructural. The unit cell contains two $[M(dmit)_2]^{2-}$ and four

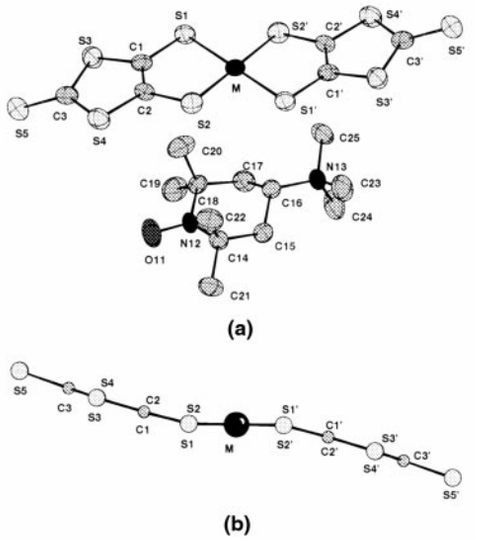

Fig. 5 (a) Molecular structure and atom labelling scheme for (Me_3N-TEMPO)$_2$[M(dmit)$_2$] (M = Ni, Pd) and (b) its side view.

Me_3N^+-TEMPO units. The structure consists of sheets of parallel $[M(dmit)_2]^{2-}$ units lying in the *ac* plane and alternating with sheets of cations along the *b* direction (Fig. S1). The two shortest distances between oxygen atoms are 7.655(2) and 7.651(3) Å. As seen on the side view of the $[M(dmit)_2]^{2-}$ shown in Fig. 5b, the molecule is not planar: the two dmit planes form an angle of 164.02(5)° (Ni) and 165.49(7)° (Pd) with the central MS_4 planar core. To our knowledge, such a chair conformation has never been observed in any other mononuclear dmit complex-based compound. Nevertheless, such a bent conformation has been observed in dinuclear compounds containing the dmit ligand together with the tto ligand (tto = $C_2S_4^{2-}$, tetrathiooxalato), namely $(R_4N)_2\{tto[Ni(dmit)]_2\}$ (R = alkyl group).[23] In these complexes, the central tto fragment forms an angle of 178 to 155.5° with the external Ni(dmit) moieties. In $(Me_3N\text{-TEMPO})_2[M(dmit)_2]$, the interplanar distance between the two dmit units is 0.868(5) Å (Ni) and 0.845(4) Å (Pd).

$(Me_3N\text{-TEMPO})[Ni(dmit)_2]$. The molecular structure, together with the atom-labelling scheme, is shown in Fig. 6. The unit cell contains four $[Ni(dmit)_2]^-$ units and four Me_3N^+-TEMPO cations. The structure consists of layers of $[Ni(dmit)_2]^-$ units lying in the *ab* plane and separated by sheets of cations along the *c* direction (Fig. 7). The layers are built on $[Ni(dmit)_2]^-$ units connected to each other through two short S···S contacts (S1···S6, 3.516(8) Å), thus forming dimers with an interplanar distance of 3.81 Å. Along the *b* direction, each dimer is connected to adjacent dimers through several S···S contacts (S4···S4: 3.519(9), S4···S5: 3.677(8), S4···S9: 3.362(6), S4···S10: 3.623(7) and S5···S9: 3.573(7) Å), thus forming chains of dimers along [010]. These chains are not isolated as they are connected to adjacent chains along the *a* direction through S1···S1 (3.614(10) Å) and S3···S7 (3.533(7) Å) contacts.

Single crystal conductivity of $(Me_3N\text{-TEMPO})[Ni(dmit)_2]$ is 4×10^{-3} S cm^{-1} at room temperature, and shows semiconductive temperature dependence ($E_a = 0.12$ eV). The rather high conductivity for a monovalent $Ni(dmit)_2$ salt can be attributed to the many short contacts between $Ni(dmit)_2$ molecules.

In the structure of the five compounds described above, the piperidine ring of the Me_3N^+-TEMPO cation adopts a chair conformation. Consequently, the six ring atoms form a very distorted plane. A useful gauge for estimating the planarity of the C_2NO moiety is given by the parameter α, which is defined[24] as the angle between the N–O bond and the CNC plane (Table 1). The C–N–C–C ($\tau 1$, $\tau' 1$), N–C–C–C ($\tau 2$, $\tau' 2$) and C–C–C–C ($\tau 3$, $\tau' 3$) torsion angles are between those observed for mono and di-substituted rings. The N–O distances and CNC angles are within the range observed in other related compounds.[25]

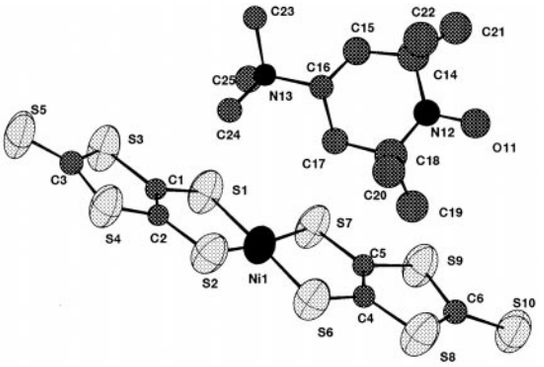

Fig. 6 Molecular structure and atom labelling scheme for $(Me_3N\text{-TEMPO})[Ni(dmit)_2]$.

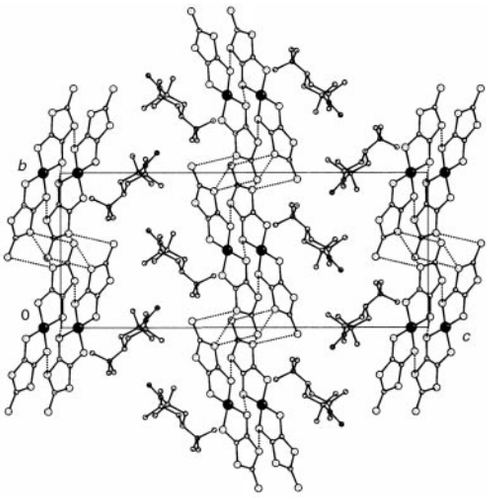

Fig. 7 Projection of the structure of $(Me_3N\text{-TEMPO})[Ni(dmit)_2]$ in the *bc* plane, showing the chains of $[Ni(dmit)_2]_2$ dimers along the *b* direction.

Magnetism

$(Me_3N\text{-TEMPO})I$ and $(Me_3N\text{-TEMPO})PF_6$. The temperature dependence of the molar magnetic susceptibility (χ) measured for a crystalline sample of $(Me_3N\text{-TEMPO})I$ is shown in Fig. 8. Within the 100–300 K temperature range, observed data are well described by the Curie–Weiss law with a Curie constant, *C*, of 0.366 emu K mol^{-1} and a Weiss constant, θ, of −6.3 K. The Curie constant corresponds to 98% of the normal value of one isolated $S = 1/2$ spin. The magnetic susceptibility exhibits a maximum at *ca.* 12 K. Below this temperature, χ decreases down to *ca.* 5 K. Upon further cooling, χ increases again. As previously indicated, some features in the crystal structure of $(Me_3N\text{-TEMPO})I$ suggest a possible dimeric arrangement. Should this compound be purely dimeric, then χ should decrease down to zero for $T \rightarrow 0$. Therefore, the behaviour below 10 K is clearly indicative of the influence of Curie impurities due to lattice defects. From the χT value extrapolated to $T = 0$, this Curie-like component is determined as $C = 0.06$ emu K mol^{-1}, which corresponds to 16% of spins. For crystals of good quality, this value is usually lower, but, in the present case, the larger value of 16% may be attributed to considerable crystal defects in the polycrystalline sample studied.

Generally, the spin density of TEMPO derivatives is mainly localized on the aminoxyl (NO) moiety.[26] ROHF/INDO calculations carried out on both $(Me_3N\text{-TEMPO})I$ and $(Me_3N\text{-TEMPO})PF_6$ confirm that the aminoxyl (NO) moiety bears at least 95% of the spin density (Fig. 9). Therefore, the magnetic properties of $(Me_3N\text{-TEMPO})I$ (and $(Me_3N\text{-TEMPO})PF_6$ as well) must essentially arise from intermolecular interactions involving the NO moieties. In $(Me_3N\text{-TEMPO})I$, the strongest interaction between NO moieties of two neighbouring radicals, A···B′ on the one hand and A···B on the other hand (see Fig. 2a) are evidenced by the short O···O distances (4.578(6) Å and 5.921(6) Å respectively; see Fig. 2a) or the even shorter corresponding N···O distances (3.789(6) Å and 5.024(6) Å, respectively). If the interaction between radicals A and B could be considered as negligible compared to that between A and B′, then $(Me_3N\text{-TEMPO})I$ could be considered as an essentially *dimeric* system. Therefore, with this assumption, the temperature dependence of the magnetic susceptibility can readily be ascribed to an antiferromagnetic coupling between $S = 1/2$ dimers, according to eqn. (1) including the corresponding term for Curie impurities:[27]

Table 1 Comparison of some geometrical features[a] of (Me_3N-TEMPO)I, (Me_3N-TEMPO)PF_6, (Me_3N-TEMPO)$_2$[Ni(dmit)$_2$], (Me_3N-TEMPO)$_2$[Pd(dmit)$_2$] and (Me_3N-TEMPO)[Ni(dmit)$_2$]

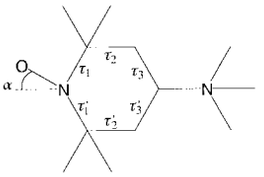

Compound	α/°	τ_1/° τ'_1/°	τ_{12}/° τ'_2/°	τ_{13}/° τ'_3/°	N–O/Å	C–N–C/°
(Me_3N-TEMPO)I	14.47	33.6(7) −34.5(7)	−47.3(6) 48.1(6)	65.5(6) −64.7(6)	1.275(5)	124.1(4)
	18.73	−35.6(7) 34.4(7)	48.0(6) −46.0(6)	−63.5(6) 62.3(6)	1.264(5)	123.6(4)
(Me_3N-TEMPO)PF_6	20.0	38.2(3)	48.1(3)	62.7(3)	1.282(4)	123.4(3)
(Me_3N-TEMPO)$_2$[Ni(dmit)$_2$]	19.82	33.9(5) −34.5(5)	−45.8(5) 46.9(5)	61.3(5) −61.9(5)	1.272(4)	124.9(3)
(Me_3N-TEMPO)$_2$[Pd(dmit)$_2$]	19.19	34.0(6) −35.0(6)	−46.3(5) 48.2(6)	63.0(6) −63.5(6)	1.273(5)	124.4(4)
(Me_3N-TEMPO)[Ni(dmit)$_2$]	14.44	40(3) −39(3)	−52(2) 50(3)	70(2) −70(2)	1.32(2)	126(2)

[a] α is the angle between the N–O bond and the C–N–C plane. τ_1, τ'_1, τ_2, τ'_2, τ_3 and τ'_3 are endocyclic torsion angles in the piperidine ring.

$$\chi = (1-\rho)\left(\frac{2N\beta^2g^2}{kT} \times \frac{1}{3+\exp\left(\frac{-J}{kT}\right)}\right) + \rho\left(\frac{NB^2g^2}{kT}\right) \quad (1)$$

where N is Avogadro's number, g is the Zeeman splitting parameter (fixed in this case at 2.00), β is the Bohr magneton, k is the Boltzman constant, J is the singlet–triplet energy gap, and ρ is the proportion of non coupled impurity. The least-square best fit is found for $J=-17.3\ cm^{-1}$ and $\rho=0.145$.[28] The agreement is satisfactory as illustrated in Fig. 8. The discrepancy factor defined as $R(\chi)=[\Sigma\ (\chi_{obs}-\chi_{calc})^2/\Sigma(\chi_{obs})^2]$ is equal to 5.2×10^{-5} in the temperature range of 5–300 K.

In the case of (Me_3N-TEMPO)PF_6, the interaction between the NO moieties of neighbouring radicals (see Fig. 4) extends over the entire crystal. The structure clearly reveals a magnetic chain of equally spaced spin $S=1/2$. The temperature dependence of the product of the magnetic susceptibility on the temperature is shown in Fig. S2. At room temperature, χT is equal to 0.328 emu K mol^{-1}, which corresponds to 88% of the expected value. The spin Hamiltonian best suited to describe the isotropic interaction between nearest neighbours is give in eqn. (2)[29]

$$H = -J\sum_{i=1}^{n-1} S_i \cdot S_{i+1} \quad (2)$$

where the summation runs over the n sites of the chain. When n tends to infinity, the results can be fitted by the numerical expression eqn. (3):[30]

$$\chi T = \left(\frac{N\beta^2g^2}{k} \times \frac{0.25+0.074975x+0.075235x^2}{1.0+0.9931x+0.172135x^2+0.757825x^3}\right) \quad (3)$$

where $x=|J|/kT$. Least squares fitting of the experimental data leads to $J=-0.17\ cm^{-1}$ with a discrepancy factor $R(\chi)$ of 9.6×10^{-6}.

Since the nature of the magnetic exchange pathway is so similar in both materials, it may appear surprising that their magnetic response is so different. Indeed, both structures reveal that the cations are placed close together and the angle between their mean planes is close to 90° (see Fig. 2 and Fig. 4). It can be inferred from these structural features that direct overlap of the NO orbitals is the sole pathway responsible for the magnetic exchange in these salts. Therefore, it can be assumed that, to a large extent, the main relevant structural parameter that correlates with the J value is the shortest N···O distance (D) between the two centres bearing the spin density. Therefore, although the Coffman expression[31] is usually used for

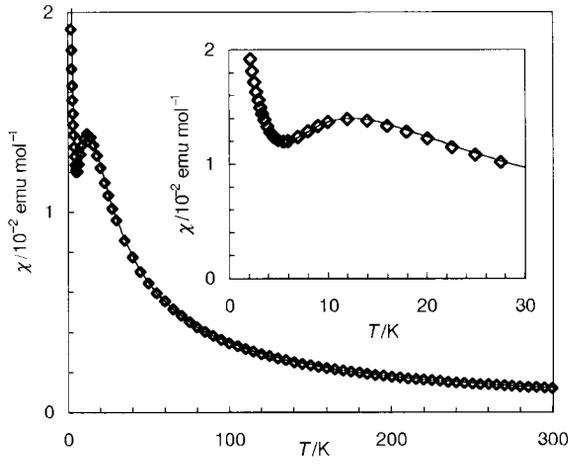

Fig. 8 Experimental (◊) and calculated (solid line) temperature dependence of the molar magnetic susceptibility of (Me_3N-TEMPO)I.

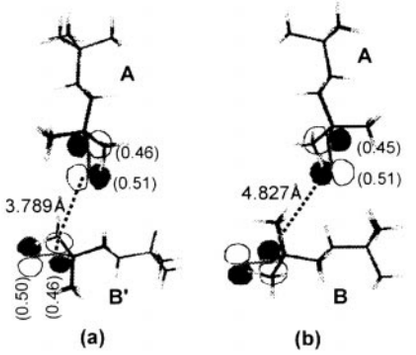

Fig. 9 Picture of the SOMO (Singly Occupied Molecular Orbital) calculated by ROHF/INDO, and views of intermolecular arrangement in (a) (Me_3N-TEMPO)I and (b) (Me_3N-TEMPO)PF_6. Numbers in round brackets are calculated spin densities on each atom in NO moiety.

intramolecular interaction, the J and D values may be tentatively analysed in the present case, with eqn. (4):

$$J = A \exp(-\varepsilon D) \quad (4)$$

where A is an appropriate exchange constant and ε is an exponential exchange coefficient. When going from $D = 3.789(6)$ to 4.827(3) Å, the present magnetic data indicate that J drops from -17.3 to $-0.17\ cm^{-1}$, which is consistent with an ε parameter equal to 4.4. This value lies in the typical 3.0–5.5 range previously reported for direct intramolecular overlaps of magnetic orbitals.[32]

The situation encountered in (Me_3N-TEMPO)I and (Me_3N-TEMPO)PF_6 contrasts with the recent report on the ferromagnetic coupling in various TEMPO-based molecules.[17b,25e,f] It should be noted that (Me_3N-TEMPO)I and (Me_3N-TEMPO)PF_6 exhibit short NO···NO distances with the NO moieties lying orthogonal to each other. This leads to non-zero overlaps, which favour antiferromagnetic interactions. By contrast, as stressed by Nogami *et al.*[17b,25e,f] TEMPO-based ferromagnetically coupled materials involves NO moieties with intermolecular NO···NO distances larger than 5.5 Å, with the corresponding orbitals being nearly parallel to each other.

(Me_3N-TEMPO)$_2$[M(dmit)$_2$] (M = Ni, Pd). In both the isostructural (Me_3N-TEMPO)$_2$[Ni(dmit)$_2$] and (Me_3N-TEMPO)$_2$[Pd(dmit)$_2$] divalent salts, the room temperature χT value is very close to the value expected for two $S = 1/2$ spin systems. Both salts show Curie behaviour without any striking magnetic interactions. This agrees with the absence of short direct distances between NO moieties in their crystal structure.

Conclusions

In this work, the great versatility of both the TEMPO radical and M(dmit)$_2$-based anion systems has been established again. Indeed, both Me_3N-TEMPO and M(dmit)$_2$ (M = Ni, Pd) can be associated in 2 : 1, 1 : 1, and even 1 : 2 non integral oxidation state salts. We have also shown that a minor chemical modification, as for example that between (Me_3N-TEMPO)I and (Me_3N-TEMPO)PF_6, may lead to a strikingly different structure and solid state properties, *i.e.*, antiferromagnetically coupled dimers for (Me_3N-TEMPO)I, antiferromagnetic chains for (Me_3N-TEMPO)PF_6. Though a number of ferromagnetic TEMPO-based compounds were recently reported,[17b,25e,f] no ferromagnetic coupling has been observed in the Me_3N^+-TEMPO-based compounds studied in this work. This may be related to the non-zero overlap of the orbitals of the NO moieties in these compounds.

The resolution of the structure of the 2 : 1 (Me_3N-TEMPO)$_2$[M(dmit)$_2$] (M = Ni, Pd) salts reveals a unique feature, *i.e.*, the chair conformation of the [M(dmit)$_2$] moieties that has never been previously observed in any known [M(dmit)$_2$]-based compound. Nevertheless, (Me_3N-TEMPO)$_2$[M(dmit)$_2$] just displays Curie behaviour, indicating no magnetic interaction between the NO moieties.

The structure of the derived 1 : 1 (Me_3N-TEMPO)[Ni(dmit)$_2$] salt consist of chains of [Ni(dmit)$_2$]$_2$ dimers connected through short S···S contacts. These S···S interactions may explain the value of the room-temperature single-crystal conductivity, $4 \times 10^{-3}\ S\ cm^{-1}$, which is rather high for a 1 : 1 integral oxidation state salt.

Preparation of further oxidised salts is in progress. As previously mentioned, an insoluble dark green powder has been obtained as a side product in the preparation of (Me_3N-TEMPO)[Ni(dmit)$_2$] by method C (see Scheme 3). Elemental analyses of this sample are consistent with a (Me_3N-TEMPO)[Ni(dmit)$_2$]$_2$ formulation. This sample has a room-temperature powder conductivity of $1 \times 10^{-2}\ S\ cm^{-1}$, and exhibits a ferromagnetic behaviour evidenced by an increase of the χT value below 100 K. Air oxidation of (Me_3N-TEMPO)$_2$[Pd(dmit)$_2$] in the presence of acetic acid afforded a black powder sample. Elemental analyses of this sample are consistent with a (Me_3N-TEMPO)[Pd(dmit)$_2$]$_4$ formulation. The room temperature powder conductivity is $1 \times 10^{-2}\ S\ cm^{-1}$.

At this stage of the work, it is clear that we have still a long way to go before obtaining compounds in this series exhibiting interplay of conductivity and magnetism. It should be however noted that, among all molecule-based material, such an interplay has been clearly established in only one series of compounds, *i.e.*, those based on the BETS donor.[6]

For ensuring interaction between conduction electrons (here, those of the M(dmit)$_2$) and localised spins, both the conducting and magnetic components should be geometrically located close to each other. Therefore the little sterically hindered nitronyl and imino aminoxyl (see Chart 1) cation radicals that are smaller and, in addition, delocalised, may be even more efficient than TEMPO-based radicals. Preparation of these ammonium cations is in progress.

Experimental

General

oxo-TEMPO was prepared from 2,2,6,6-tetramethyl-4-piperidone or its hydrochloride.[33] (n-Bu_4N)$_2$[Ni(dmit)$_2$], (n-Bu_4N)-[Ni(dmit)$_2$] and (n-Bu_4N)$_2$[Pd(dmit)$_2$] were prepared following previously reported methods.[34] Other starting materials used in this work were used without further purification unless otherwise noted. New compounds were characterised from single-crystal structure by X-ray analysis, or elemental analysis data are given.

(Me_3N-TEMPO)I

Me_2N-TEMPO was prepared by reductive amination[35] of oxo-TEMPO (13.8 g, 81.0 mmol). Crude Me_2N-TEMPO dissolved in ethanol (100 cm^3) was reacted with methyl iodide (11.0 g, 77.2 mmol). This afforded the (Me_3N-TEMPO)I ammonium salt as pale orange microcrystals (10.8 g, 31.7 mmol) in a 40% yield.[36] Single crystals were obtained by slow evaporation of acetonitrile solutions.

(Me_3N-TEMPO)PF_6

Filtered solutions of (Me_3N-TEMPO)I (3.67 g, 10.8 mmol) in water (100 cm^3) and KPF_6 (27.0 g, 147 mmol) in water (200 cm^3) were mixed together. Pale orange microcrystals immediately formed, which were filtered off and washed with ethanol and ether to afford 3.46 g (9.63 mmol) of (Me_3N-TEMPO)PF_6 in a 89% yield. Single crystals were obtained by slow evaporation of acetonitrile solutions.

(Me_3N-TEMPO)$_2$[Ni(dmit)$_2$]

Method A. Filtered solutions of (Me_3N-TEMPO)I (1.00 g, 2.93 mmol) in acetonitrile (200 cm^3) and (n-Bu_4N)$_2$[Ni(dmit)$_2$] (0.642 g, 0.664 mmol) in acetone (180 cm^3) were mixed together, and left for a week. Filtration and washing with acetonitrile and acetone afforded deep dark violet blocks (0.381 g, 0.433 mmol; typical dimensions were $0.3 \times 0.2 \times 0.2\ mm^3$) in a 65% yield.

Method B. Na_2(dmit) was generated *in situ* from dmit-$(COPh)_2$ (0.541 g, 1.33 mmol) and CH_3ONa (0.439 g, 8.13 mmol) in methanol (10 cm^3). To the resulting mixture, solutions of $NiCl_2 \cdot 6H_2O$ (0.166 g, 0.697 mmol) in methanol (20 cm^3) and (Me_3N-TEMPO)I (0.386 g, 1.13 mmol) in 95% methanol (65 cm^3) were successively added. After stirring overnight, a dark green crystalline powder was filtered off, redissolved in acetone–acetonitrile, and reprecipitated with

Table 2 Crystallographic data for (Me_3N-TEMPO)I, (Me_3N-TEMPO)PF_6, (Me_3N-TEMPO)$_2$[Ni(dmit)$_2$], (Me_3N-TEMPO)$_2$[Pd(dmit)$_2$] and (Me_3N-TEMPO)[Ni(dmit)$_2$]

	Compound				
Chemical formula	$C_{24}H_{52}I_2N_4O_2$	$C_{12}H_{26}F_6N_2OP$	$C_{30}H_{52}N_4O_2NiS_{10}$	$C_{30}H_{52}N_4O_2PdS_{10}$	$C_{18}H_{26}N_2ONiS_{10}$
Formula weight	682.50	359.32	880.06	927.76	665.72
T/K	293(2)	160(2)	293(2)	293(2)	293(2)
Crystal system	monoclinic	orthorhombic	orthorhombic	orthorhombic	monoclinic
Space group	$P2_1/n$	*Pnma*	*Pbca*	*Pbca*	$P2_1/c$
a/Å	14.437(4)	11.400(1)	14.521(2)	14.646(3)	8.372(1)
b/Å	13.763(4)	10.852(1)	15.982(3)	16.012(4)	11.998(2)
c/Å	17.278(4)	13.354(2)	18.150(5)	18.126(5)	28.592(4)
β/°	112.45(2)	—	—	—	91.25(2)
V/Å^3	3173(2)	1652.1(3)	4212(1)	4250(2)	2871.2(7)
ρ_{calcd}/g cm^{-3}	1.429	1.445	1.388	1.450	1.540
Z	4	4	4	4	4
μ(Mo-K$_\alpha$)/mm^{-1}	2.006	0.229	0.989	0.960	1.419
Reflections collected/unique	9478/9161	15600/1676	7420/1957	5550/5527	27237/5644
R_{int}	0.0717	0.0534	0.0645	0.0113	0.2928
$R(F_o)^a$	0.0327	0.0453	0.0271	0.0401	0.0715
$R_w(F_o)^b$	0.1191	0.1130	0.0525	0.1048	0.1551

$^a R(F_o) = \Sigma(||F_o|-|F_c||)/\Sigma|F_o|$. $^b R_w(F_o) = [\Sigma w(|F_o|-|F_c|)^2/\Sigma wF_o^2]^{1/2}$.

propan-2-ol to afford dark purple microcrystals (0.378 g, 0.429 mmol) in a 65% yield. Found: C, 41.07; H, 5.52; N, 6.31%; ($C_{12}H_{26}N_2O)_2(NiC_6S_{10}$) requires C, 40.94; H, 5.96; N, 6.37%.

(Me_3N^+-TEMPO)$_2$[Pd(dmit)$_2$]

Method A. Filtered solutions of (Me_3N-TEMPO)I (0.494 g, 1.45 mmol) in acetonitrile (60 cm^3) and (n-$Bu_4N)_2$[Pd(dmit)$_2$] (0.323 g, 0.328 mmol) in acetone (50 cm^3) were mixed together, and left at room temperature for one day. Filtration and washing with acetonitrile and acetone afforded deep violet blocks (0.142 g, 0.153 mmol, typical dimensions $0.3 \times 0.2 \times 0.1$ mm^3) in a 47% yield. A second crop (0.108 g) is obtained after concentration of the resulting solution.

Method B. Na_2(dmit) was generated *in situ* from dmit-$(COPh)_2$ (0.429 g, 1.09 mmol) and CH_3ONa (0.325 g, 6.02 mmol) in methanol (10 cm^3). To the resulting mixture, solutions of K_2PdCl_4 (0.190 g, 0.582 mmol) in 50% aq. methanol (20 cm^3) and (Me_3N-TEMPO)I (0.368 g, 1.08 mmol) in 95% methanol (100 cm^3) were successively added. After stirring overnight, a dark red-violet powder was filtered off, redissolved in acetone–acetonitrile, and reprecipitated with propan-2-ol to afford dark purple microcrystals (0.219 g, 0.236 mmol) in a 44% yield. Found: C, 38.66; H, 5.27; N, 5.87%; ($C_{12}H_{26}N_2O)_2(PdC_6S_{10}$) requires C, 38.83; H, 5.65; N, 6.04%.

(Me_3N-TEMPO)[Ni(dmit)$_2$]

Method C. Na_2[Ni(dmit)$_2$] was prepared *in situ* from Na_2(dmit) (0.300 g, 1.23 mmol) in acetone (30 cm^3) and $NiCl_2 \cdot 6H_2O$ (0.161 g, 6.76 mmol) in MeOH (7 cm^3). Iodine (0.038 g, 0.150 mmol) in acetone (30 cm^3) and (Me_3N-TEMPO)I (0.234 g, 0.682 mmol) in MeOH (30 cm^3) were successively added. The solution was concentrated to half volume and placed in a freezer. Addition of *i*-PrOH gave a mixture of a brown powder and black shiny needles. These needles were characterised as the monovalent (Me_3N-TEMPO)[Ni(dmit)$_2$] salt by X-ray analysis.

Method D. A solution of iodine (0.0363 g, 0.143 mmol) in acetone (30 cm^3) was added to a solution of (Me_3N-TEMPO)$_2$[Ni(dmit)$_2$] (0.245 g, 0.278 mmol) in acetone (1 dm^3). After 2 days, the reaction mixture was concentrated down to 25 cm^3 and filtered to remove (Me_3N-TEMPO)I formed during this reaction. The filtrate was reprecipitated by adding ether (100 cm^3) to give crude (Me_3N-TEMPO)[Ni(dmit)$_2$]. Recrystallisation from acetone yielded dark green needles and micro-crystals (0.139 g, 0.209 mmol) in a 75% yield. Found: C, 31.14; H, 2.86; N, 4.47%; ($C_{12}H_{26}N_2O)(PdC_6S_{10}$) requires C, 32.47; H, 3.94; N, 4.21%.

Electrochemical studies

Cyclic voltammetry data (homemade potentiostat interfaced with a PC computer):[37] Au working microelectrode (125 μm), acetonitrile solution, 0.1 mol dm^{-3} (n-$Bu_4N)ClO_4$ as supporting electrolyte (dried by melting and pumping under vacuum immediately before use), Pt wire as auxiliary electrode, SCE as reference electrode. Square wave voltammetry[38] data were recorded on a PAR273.

X-Ray diffraction

For (Me_3N-TEMPO)I and (Me_3N-TEMPO)$_2$[M(dmit)$_2$] (M = Ni, Pd), data collection was carried out on a Enraf-Nonius CAD4 diffractometer with graphite-monochromated Mo-Kα radiation ($\lambda = 0.71073$ Å) by using the CAD4-Express package.[39] For every compound, the intensity of three reflections was monitored throughout the data collection, and no significant decay was observed. Accurate unit cell parameters were obtained by least-squares refinements on the basis of the setting angles of 25 reflections. Empirical absorption corrections based on psi-scans were applied for every compound.[40]

For (Me_3N-TEMPO)PF_6 and (Me_3N-TEMPO)[Ni(dmit)$_2$], data collection and cell refinement were performed on a IPDS Stoe diffractometer, by using the IPDS software[41] at 160 and 293 K, respectively. All calculations were carried out using the WinGX package (version 1.62),[42] with SIR92[43] or SHELXS86[44] for the structure solution and SHELXL97[45] for the subsequent refinements. Drawings were obtained with CAMERON.[46]

All non-H atoms were refined anisotropically, except in (Me_3N-TEMPO)[Ni(dmit)$_2$], for which C, N and O were refined isotropically. Positions of H atoms were calculated, with an isotropic displacement parameter 20% higher than that of the parent atom. Crystallographic data for every compound are summarised in Table 2. CCDC reference number 1145/260. See http://www.rsc.org/suppdata/jm/b0/b008424g/ for crystallographic files in .cif format.

Conductivity measurements

Temperature dependent single-crystal conductivity measurements were carried out following the standard four-probe technique. Electrical contacts were obtained by gluing four gold wires to the crystal with Emetron M8001 gold paint.

Magnetic measurements

Static magnetic measurements were carried out using a Quantum Design MPMS 5S SQUID magnetometer with the temperature range of 1.8–300 K and 0–5 T for randomly oriented crystals. The samples were contained in a thin plastic wrap (New Krewrap®, Kureha Chemicals Industry Co., Ltd.). The diamagnetic contribution of the sample holder was corrected experimentally. The diamagnetic contributions (χ_{dia}) of the constituent atoms were experimentally determined. $\chi_{dia}/10^{-6}$ emu mol^{-1}; (Me_3N-TEMPO)I, −185; (Me_3N-TEMPO)PF_6 −190; (n-Bu_4N)$_2$[Ni(dmit)$_2$], −580; (n-Bu_4N)$_2$[Pd(dmit)$_2$], −539; (n-Bu_4N)Br, −203. From these values and Pascal's constants for I^- and Br^-, determined as Me_3N^+-TEMPO, –133; [Ni(dmit)$_2$]$^{2-}$, −246; [Pd(dmit)$_2$]$^{2-}$, −205.

Semiempirical computations

The INDO (intermediate neglect of differential overlap)[47] method was employed for the calculation of the molecular orbitals of Me_3N^+-TEMPO. Calculations were performed using ZINDO with the INDO/1 Hamiltonian in the CAChe work system.[48] As Me_3N^+-TEMPO is paramagnetic, the restricted open-shell Hartree–Fock (ROHF) formalism was adopted. Metrical parameters used for the calculation were taken from the present crystal structures.

Acknowledgements

Printed circuits for conductivity measurements were kindly supplied by the Motorola Company. We thank D. de Montauzon for assistance in electrochemical studies. This research was supported in part (YH and KI) by a Grant-in-Aid for Scientific Research on Priority Area (B) of Molecular Conductors and Magnets (Area No. 730/11224214) from the Ministry of Education, Science, Sports and Culture, Japan.

References

1 H. Kobayashi, A. Kobayashi and P. Cassoux, *Chem. Soc. Rev.*, 2000, **29**, 325.
2 P. Day, M. Kurmoo, T. Mallah, I. R. Marsden, R. H. Friend, F. L. Platt, W. Hayes, D. Chasseau, J. Gaultier, G. Bravic and L. Ducasse, *J. Am. Chem. Soc.*, 1992, **114**, 10722.
3 E. Coronado, L. R. Falvello, J. R. Galán-Mascarós, C. Giménez-Saiz, C. J. Gómez-García, V. N. Lauhkin, A. Pérez-Benítez, C. Rovira and J. Veciana, *Adv. Mater.*, 1997, **9**, 984.
4 For a review, see R. Kato, *Bull. Chem. Soc. Jpn.*, 2000, **73**, 515.
5 M. Kurmoo, A. W. Graham, P. Day, S. J. Coles, M. B. Hursthouse, J. L. Caufield, J. Singleton, P. L. Pratt, W. Hayes, L. Ducasse and P. Guionneau, *J. Am. Chem. Soc.*, 1995, **117**, 12209.
6 L. Brossard, R. Clerac, C. Coulon, M. Tokumoto, T. Ziman, D. K. Petrov, V. N. Laukhin, M. J. Naughton, A. Audouard, F. Goze, A. Kobayashi, H. Kobayashi and P. Cassoux, *Eur. Phys. J. B*, 1998, **1**, 439.
7 E. Ojima, H. Fujiwara, K. Kato, H. Kobayashi, H. Tanaka, A. Kobayashi, M. Tokumoto and P. Cassoux, *J. Am. Chem. Soc.*, 1999, **121**, 5581.
8 P. Cassoux and L. Valade, in *Inorganic Materials*, eds. D. W. Bruce and D. O'Hare, 2nd edn., John Wiley & Sons, New York, 1996, pp. 1–64, and references therein.
9 P. Cassoux and J. Miller in *Chemistry of Advanced Materials: An Overview*, eds. L. V. Interrante and M. J. Hampden-Smith, VCH Publishers, New York, 1997, pp. 19–72, and references therein.
10 J. S. Miller, A. J. Epstein and W. M. Reiff, *Mol. Cryst. Liq. Cryst.*, 1985, **120**, 27.
11 J. S. Miller and A. J. Epstein, *Chem. Eng. News*, 1995, **73**, 30.
12 C. Faulmann, A. E. Pullen, E. Riviere, Y. Journaux, L. Retailleau and P. Cassoux, *Synth. Met.*, 1999, **103**, 2296.
13 For a review, see M. Kinoshita, *Jpn. J. Appl. Phys.*, 1994, **33**, 5718.
14 IUPAC recommended name is 2-(*p*-nitrophenyl)-4,4,5,5-tetramethyl-4,5-dihydro-1*H*-imidazol-1-oxyl 3-oxide.
15 M. Tamura, Y. Nakazawa, D. Shiomi, K. Nozawa, Y. Hosokoshi, M. Ishikawa, M. Takahashi and M. Kinoshita, *Chem. Phys. Lett.*, 1991, **186**, 401; Y. Nakazawa, M. Tamura, N. Shirakawa, D. Shiomi, M. Takahashi, M. Kinoshita and M. Ishikawa, *Phys. Rev. B: Condens. Matter*, 1992, **46**, 8906.
16 R. Chiarelli, M. A. Novak, A. Rassat and J. L. Tholence, *Nature (London)*, 1993, **363**, 147.
17 (*a*) K. Togashi, R. Imachi, K. Tomioka, H. Tsuboi, T. Ishida, T. Nogami, N. Takeda and M. Ishikawa, *Bull. Chem. Soc. Jpn.*, 1996, **69**, 2821; (*b*) T. Nogami, T. Ishida, M. Yasui, F. Iwasaki, N. Takeda, M. Ishikawa, T. Kawakami and K. Yamaguchi, *Bull. Chem. Soc. Jpn.*, 1996, **69**, 1841.
18 See for example: Y. Mazaki, K. Awaga and K. Kobayashi, *J. Chem. Soc., Chem Commun.*, 1992, 1661; S. Nakatsuji, A. Takai, K. Nishikawa, Y. Morimoto, N. Yasuoka, K. Suzuki, T. Enoki and H. Anzai, *Chem. Commun.*, 1997, 275; S. Nakatsuji, A. Takai, K. Nishikawa, Y. Morimoto, N. Yasuoka, K. Suzuki, T. Enoki and H. Anzai, *J. Mater. Chem.*, 1999, **9**, 1747.
19 H. Imai, T. Inabe, T. Otsuka, T. Okuno and K. Awaga, *Phys. Rev. B*, 1996, **54**, R6838; H. Imai, T. Otsuka, T. Naito, K. Awaga and T. Inabe, *J. Am. Chem. Soc.*, 1999, **121**, 8098.
20 The IUPAC recommended name for the NO radical moiety is aminoxyl. The terms nitroxide and nitroxyl are also conventionally used.
21 (*a*) T. Sugimoto, S. Yamaga, M. Nakai, M. Tsuji, H. Nakatsuji and N. Hosoito, *Chem. Lett.*, 1993, 1817; (*b*) R. Kumai, M. Matsushita, A. Izuoka and T. Sugawara, *J. Am. Chem. Soc.*, 1994, **116**, 4523; (*c*) S. Nakatsuji, N. Akashi, K. Suzuki, T. Enoki, N. Kinishita and H. Anzai, *Mol. Cryst. Liq. Cryst.*, 1995, **268**, 153; (*d*) S. Nakatsuji, A. Hirai, J. Yamada, K. Suzuki, T. Enoki and H. Anzai, *Mol. Cryst. Liq. Cryst.*, 1997, **306**, 409; (*e*) H. Fujiwara and H. Kobayashi, *Synth. Met.*, 1999, **102**, 1740.
22 For a review, see S. Nakatsuji and H. Anzai, *J. Mater. Chem.*, 1997, **7**, 2161.
23 A. E. Pullen, R.-M. Olk, S. Zeltner, E. Hoyer, K. A. Abboud and J. R. Reynolds, *Inorg. Chem.*, 1997, **36**, 958; A. E. Pullen, S. Zeltner, R.-M. Olk, E. Hoyer, K. A. Abboud and J. R. Reynolds, *Inorg. Chem.*, 1997, **36**, 4163.
24 J. Lajzerowicz-Bonneteau in *Spin labeling: Theory and Applications*, ed. L. J. Berliner, Academic Press, New York, 1976, pp. 239–249.
25 (*a*) M. Le Bars-Combe, *Acta Crystallogr. Sect. B*, 1982, **38**, 2749; (*b*) F. A. Cotton and T. R. Felthouse, *Inorg. Chem.*, 1982, **21**, 2667; (*c*) M. Cygler, *Can. J. Chem.*, 1982, **60**, 2392; (*d*) F. Lanfranc de Panthou, D. Luneau, J. Laugier and P. Rey, *J. Am. Chem. Soc.*, 1993, **115**, 9095; (*e*) F. Iwasaki, J. H. Yoshikawa, H. Yamamoto, K. Takada, E. Kan-Nari, M. Yasui, T. Ishida and T. Nogami, *Acta Crystallogr., Sect. B*, 1999, **55**, 231; (*f*) F. Iwasaki, J. H. Yoshikawa, H. Yamamoto, E. Kan-Nari, K. Takada, M. Yasui, T. Ishida and T. Nogami, *Acta Crystallogr., Sect. B*, 1999, **55**, 1057.
26 D. Bordeaux, J. X. Boucherle, B. Delley, B. Gillon, E. Ressouche and J. Schweizer in *Magnetic Molecular Materials (NATO ASI Series. Series E, Applied Science - vol. 198)*, eds. D. Gatteschi, O. Kahn, J. S. Miller and F. Palacio, Kluwer Academic Publishers, Dordrecht, 1991, pp. 371–383.
27 B. Bleaney and K. D. Bowers, *Proc. R. Soc. London, Ser. A*, 1952, **A214**, 451.
28 This ρ value of 0.145 is in good agreement with the experimental estimation of 16% of impurities.
29 O. Kahn, *Molecular Magnetism*, VCH Publishers, New York, 1993.
30 W. E. Estes, D. P. Gavel, W. E. Hatfield and D. J. Hodgson, *Inorg. Chem.*, 1978, **17**, 1415.
31 R. E. Coffman and G. R. Buettner, *J. Phys. Chem.*, 1979, **83**, 2387.
32 See for example: (*a*) J. Kondo, *Solid State Phys.*, 1969, **23**, 183; (*b*) A. Niemann, U. Bossek, K. Wiegardt, C. Butzlaff, A. X. Trautwein and B. Nuber, *Angew. Chem., Int. Ed. Engl.*, 1992, **31**, 311.
33 S. Banerjee and G. K. Trivedl, *Tetrahedron*, 1992, **48**, 9939.
34 G. Steimecke, H.-J. Sieler, R. Kirmse and E. Hoyer, *Phosphorus Sulfur Relat. Elem.*, 1979, **7**, 49.
35 *Organic Synthesis*, John Wiley & Sons, New York, 1998, Coll. vol. 6, pp. 499–501.
36 This compound can be also prepared from MeNH–TEMPO and

MeI: E. J. Rauckman, G. M. Rosen and W. W. Hord, *Org. Prep. Proced. Int.*, 1977, **9**, 53.
37 P. Cassoux, R. Dartiguepeyron, P.-L. Fabre and D. de Montauzon, *Actual. Chim.*, 1985, 79; P. Cassoux, R. Dartiguepeyron, P.-L. Fabre and D. de Montauzon, *Electrochim. Acta*, 1985, **11**, 1485.
38 L. Ramaley and M. S. Krause Jr, *Anal. Chem.*, 1969, **41**, 1362.
39 CAD4 Express Software. Enraf-Nonius, Delft, The Netherlands, 1994.
40 A. C. T. North, D. C. Phillips and F. S. Mathews, *Acta. Crystallogr., Sect. A*, 1968, **24**, 351.
41 IPDS Software, version 2.86, Stoe & Cie, Darmstadt, Germany, 1996.
42 WINGX Main Reference, L. J. Farrugia, *J. Appl. Crystallogr.*, 1999, **32**, 837.
43 A. Altomare, G. Cascarano, C. Giacovazzo and A. Guagliardi, *J. Appl. Crystallogr.*, 1993, **26**, 343.
44 G. M. Sheldrick, *Program for Crystal Structure Solution*, Germany, 1986.
45 G. M. Sheldrick, *Programs for Crystal Structure Analysis (Release 97-2)*, Göttingen, Germany, 1998.
46 D. M. Watkin, L. Pearce and C. K. Prout, *CAMERON — A Molecular Graphics Package*, Chemical Crystallography Laboratory, University of Oxford, 1993.
47 (*a*) M. Zerner, G. Loew, R. Kirchner and U. Mueller-Westerhoff, *J. Am. Chem. Soc.*, 1980, **102**, 589; (*b*) W. P. Anderson, D. Edwards and M. C. Zerner, *Inorg. Chem.*, 1986, **25**, 2728.
48 The MO calculations were performed using CAChe version 3.8, CAChe Scientific Inc., 1995.